Large tailorable range in optical properties of GeS_2-Sb_2S_3 chalcogenide glasses

YANYING LI[a], CHANGGUI LIN[a,b*], ZHUOBIN LI[b], FEILI WANG[b]
[a]*The School of Materials Science & Chemical Engineering, Ningbo University, Ningbo 315211, Zhejiang, P.R. China*
[b]*Laboratory of Infrared Materials and Devices, Ningbo University, Ningbo 315211, Zhejiang, P.R. China*

We prepared GeS_2-Sb_2S_3 chalcogenide glasses and investigated the compositional dependence of their linear and nonlinear optical properties. The results showed that large variation range of optical bandgap, linear refractive index, volume of structural nano-voids, and nonlinear optical response (n_2 and β) was achieved within this sole glass-forming region. The role of Sb_2S_3 addition in these properties was also discussed from the microstructural view. It would be of reference significance for comparing or selecting chalcogenide glasses with suitable optical properties for applications in infrared spectral region.

(Received November 28, 2011; accepted September 20, 2012)

Keywords: Chalcogenide glass, Optical properties, Z-scan, Third-order optical nonlinearity

1. Introduction

Intriguing properties of chalcogenide glasses such as wide transparency window extending to mid-infrared (IR), photosensitivity, and large optical nonlinearities, are attractive for important optoelectronic applications as new generation IR optical and memory devices [1-4]. In practical photonic integration, many of the attributes of chalcogenide glasses are particularly compelling, e.g. viscosity, linear refractive index, nonlinear refractive index and absorption. Fortunately, a great advantage of the glass is the adjustability of physicochemical properties, which can be continuously tailored by compositional control within glass-forming region. Thus, the possibility of controlling the attributes of chalcogenide glasses in a large variable range is of significance in the realization of optimal IR photonic elements matchable with the present or novel optoelectronic system.

In binary or pseudo-binary sulfide glasses, various kinds of glass systems have been intensively studied with focus on their physicochemical properties, including Ge-S, As-S, and Ge-M-S (M=Ga, As, Sb, or In) systems [5-10]. Among them, the Ge-Sb-S system is one of the most attractive because of its large glass-forming region [6, 11] and flexible thermal properties [6, 12-15]. Especially, it is impressive that a large compositional dependence of glass transition temperature T_g and T_x-T_g (T_x, the onset crystallization temperature) can be achieved ranging from 200 °C to 500 °C and ~20 °C to 220°C, respectively, indicating flexible thermal stability and the contradictory possibility of either fiber drawing [14] or controllable crystallization [6] in Ge-Sb-S glass system. This can be roughly ascribed to the big difference of bonding and microstructural arrangement between SbS_3 pyramidal and GeS_4 tetrahedral units [6, 16]. Therefore, a large compositional dependence of optical properties also could be expected in stoichiometric GeS_2-Sb_2S_3 glasses, making it attractive for different optical applications. However, few investigations were focused on their optical properties [17]. In this study the compositional dependences of linear and nonlinear optical properties in GeS_2-Sb_2S_3 glasses are studied and large tailorability is realized by comparing with that of other glass systems, such as GeS_2-Ga_2S_3 and GeS_2-In_2S_3.

2. Experimental

Bulk glassy samples of (100-x)GeS_2-xSb_2S_3 (x=0, 10, 20, 30, 40, 50, 60, 70, 80, and 90) were synthesized by melt quenching of the mixture of high purity (99.999%) Ge, Sb, and S elements. Hereinafter, GSx was delegated the composition of GeS_2-Sb_2S_3 glasses. Appropriate quantity of these raw materials was sealed in evacuated quartz ampoules (~10^{-3} Pa), and then rocked at 920-980 °C for 18h in order to obtain the homogenous chalcogenide glass samples. After water quenching, the ampoules were annealed at a temperature of 10-20 °C below the T_g to remove mechanical strains. Finally, glass disks (Φ10 mm×1 mm) were sliced from the glass rods and polished to optical quality on both sides for optical measurements.

The visible and near-IR (Vis-NIR) absorption spectra of the glasses were recorded with a PerkinElmer-LAMBDA 950 UV/VIS/NIR spectrophotometer over a spectral range from 400 to 2500 nm. And mid-IR transmission measurement was done with a FT-IR spectroscopy (Thermo Nicolet, Nexus 380) in the range from 400 to 4000 cm^{-1}. Linear refractive indices (n_0) were measured by a prism-coupling technique (Korean, SAIRON SPA 4000) with laser wavelength of 633 nm. For the refractive index measurement of GSx glasses, only can the x smaller than 30 be measured because of the limitation of the refractive index of coupled prism. The third-order optical nonlinearities (including the magnitude and sign of the nonlinear refractive index n_2

and nonlinear absorption coefficient β) were measured by a conventional Z-scan method under excitation wavelength of 800 nm. Excitation is provided by a Ti : Sapphire laser system (Coherent Mira 900-D) that generates ultra-short laser pulses of 200 fs with a repetition rate of 76 MHz. The detailed experimental setup was described in Ref. [18]. All the above measurements were performed at room temperature.

3. Results and discussion

The photos and Vis-NIR absorption spectra of the GSx glasses are presented in Fig. 1 a) and b), respectively. It is obvious that the color of glass samples changes from yellowish orange to red, and then to opaque black to human eyes. And it is in good accordance with the variation of absorption edge of short wavelength as displayed in Fig. 1 b). The quantitative characteristic of optical bandgap (defined as when absorbance is 1) corresponding to these spectra are collected in Table 1. Compared with that of GeS_2-Ga_2S_3 glasses as indicated in Fig. 2, a wider variable range of optical bandgap is suggested in GSx glasses. Similar phenomenon also can be observed for the behavior of refractive index n_0, which ranges from 2.1188 to 2.4458 for only 30 mol% variation of Sb_2S_3 content. It can be attributed to the different degrees of impact between Sb and Ga on the band structure and electron density or polarizability of ions. In this case, the Sb^{3+} ions act as electron deficiency by forming dative bonds with the S lone pairs [19], and meanwhile possess larger polarizability than that of Ge^{4+} and Ga^{4+} ones [20]. Consequently, compared with the substitution of [GaS_4] tetrahedral units for [GeS_4] ones in GeS_2-Ga_2S_3 glasses, the higher energy of the electronic states at the top of the valence band and larger polarizability of ions are achieved simultaneously for the substitution of electron deficiency units of [SbS_3] pyramid in GSx glasses [6, 16, 19].

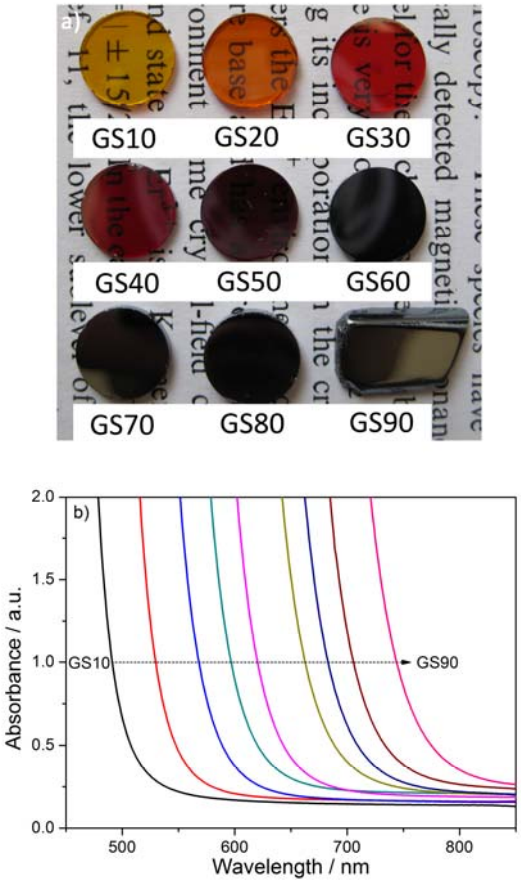

Fig. 1 a) Photographs and b) Vis-NIR absorption spectra of GSx glasses: GS10, GS20, GS30, GS40, GS50, GS60, GS70, GS80, and GS90, respectively.

Table 1 Some optical parameters of GSx glasses.

Glass samples	Optical bandgap, Eg [eV]	Refractive index, n @ 632.8 nm	Nonlinear refractive index, n_2 [$\times 10^{-17} m^2/W$]	Nonlinear absorption coefficient, β [$\times 10^{-10} m/W$]
GS0	2.70	2.1188	-	-
GS10	2.53	2.2273	6.89	1.16
GS20	2.34	2.3348	9.33	4.24
GS30	2.18	2.4458	19.9	5.55
GS40	2.08	-	31.0	8.64
GS50	2.00	-	34.0	11.5
GS60	1.87	-	38.4	11.3
GS70	1.81	-	23.7	15.6
GS80	1.76	-	25.5	19.5
GS90	1.67	-	50.5	104

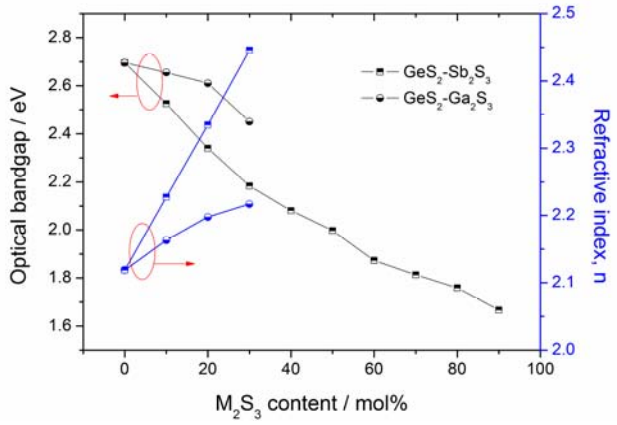

Fig. 2 Compositional trends in optical bandgap and linear refractive index of GeS_2-Ga_2S_3 and GSx glasses.

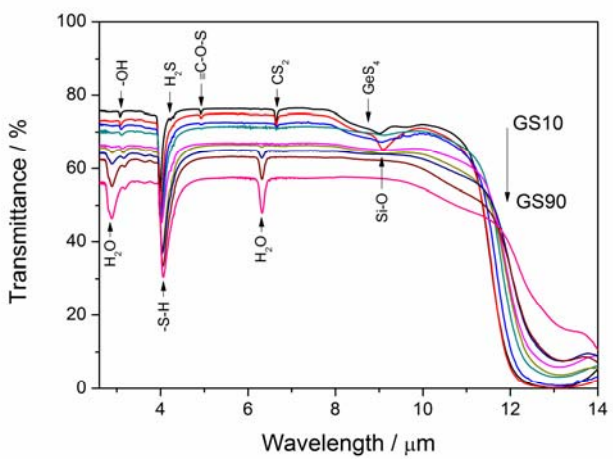

Fig. 3 Mid-IR transmission spectra of GSx glasses.

Fig. 3 shows the mid-IR transmission spectra of the GSx glasses, and the related impurity absorption bands are also identified according to the previous experimental results [21, 22]. It is interesting to note that the intensity, the spectral position and the form of all impurity absorption bands strongly depend on their glass composition. As indicated in Fig. 3, the absorption bands at 4.9, 6.6, and 8.7 μm are ascribed to the vibration of ≡C-O-S, CS_2, and GeS_4 bonds, respectively. These impurity bands might be caused by the pollution of the initial raw materials, especially Ge as discussed elsewhere [21], because they are gradually vanishing in the glasses with low Ge content. The disappearance of Si-O band at 9.1μm is mainly due to the decreasing temperature of synthesis from 980 °C to 920 °C, reducing the disintegration of SiO_2 amorphous layer on the inner surface of silica ampoule [22]. Another notable phenomenon is the molecular-adsorbed water bands located at 2.9 and 6.3μm drops abruptly when x more than 50 in GeS_2-Sb_2S_3 glasses, and grows gradually. This feature may be correlated to the structural evolution from the compact connectivity of four-coordinated Ge species to the loosen connectivity of three-coordinated Sb entities. We assumed that when the addition of Sb_2S_3 content exceed to 50%, the initial 3D glass network would be transformed to 2D structure, which was responsible for the appearance of nanovoids adsorbing water molecule [17, 22]. More specific investigation on the large structural fluctuation with the increasing Sb_2S_3 content is in progress.

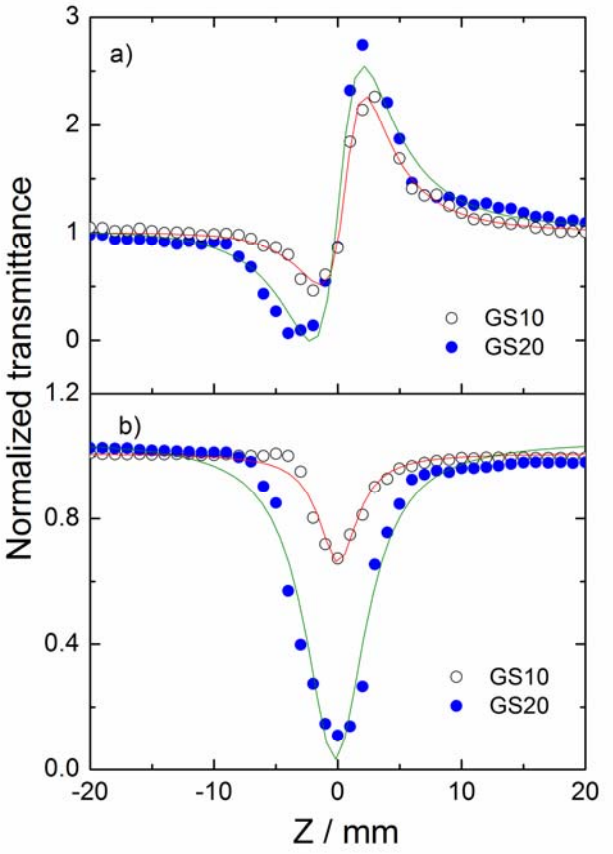

Fig. 4 Normalized transmittance as a function of the position of the GS10 and GS20 glass samples in the closed a) and open b) aperture scheme under the excitation wavelength of 800 nm, respectively.

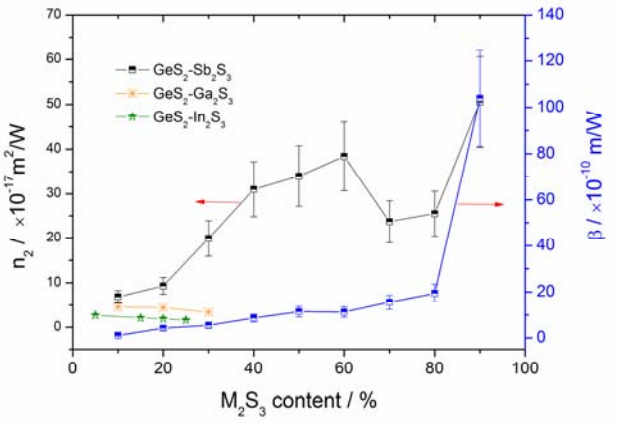

Fig. 5 Compositional dependence in GSx glasses of nonlinear refractive index, n_2 and nonlinear absorption coefficient, β, respectively. The nonlinear optical susceptibilities $\chi^{(3)}$ of GeS_2-Ga_2S_3 ($\times 10^{-13}$ esu) [29] and GeS_2-In_2S_3 ($\times 10^{-13}$ esu) [9] are also presented for comparison.

Nonlinear refraction and nonlinear absorption were investigated using the conventional Z-scan technique at 800 nm. Fig. 4 a) and b) show typical close- and open-aperture Z-scan traces for GS10 and GS20 samples, respectively. The solid lines are the best-fit curves obtained using the procedure of Ref. [23]. The values of n_2 and β listed in Table 1, determined with an estimated error of 20%, are plotted in Fig. 5 as a function of the Sb_2S_3 content. The two-photon absorption coefficient β shows a rising trend with increasing content of Sb_2S_3, and a steep edge around 90% Sb_2S_3 content is observed. We have demonstrated that an increase Sb_2S_3 shifts the absorption bandgap to infrared as shown in Fig. 1. Consequently, this two photon absorption process is governed by the decreasing band energy E_g with a form of $h\omega/E_g$, where $h\omega$ is incident photon energy. The exponential shape of β displayed in Fig. 5 implies that it is resonantly enhanced by the gap states [24] where located at $h\omega/E_g$~0.93. One can also see in Fig. 5 a similar growing trend of nonlinear refractive index n_2 in comparison with that of β, except a bump with a maximum located at 60% Sb_2S_3 (of ~0.83 $h\omega/E_g$). It has been believed that this growing trend is not only dependent on the resonant enhancement of two-photon absorption, but also on the lone electron pairs concentration which increases with the addition of SbS_3 [25, 26]. Additionally, the behavior of n_2 also is mainly determined by normalized photon energy $h\omega/E_g$, described by the Sheik-Bahae relation $n_2 n_0 = KG(h\omega/E_g)/E_g^4$, where K is a fixed constant and $G(h\omega/E_g)$ is a spectral function [27]. For an ideal amorphous semiconductor, n_2 is maximal at $h\omega/E_g$=0.5. Nevertheless, the band tail states in chalcogenide glasses cause a large deviation of spectral dependence of intensity-dependent refractive index n_2 in this study [28]. Consequently, it is assumed to be responsible for the broad peak in a range of normalized photon energy $0.66<h\omega/E_g<0.85$. Aside from the mechanism discussion of these nonlinear optical processes, more importantly, the n_2 of the studied GSx glasses shows a larger variation range, which is given by nearly an order of magnitude, compared with the small n_2 variation of GeS_2-In_2S_3 [9] and GeS_2-Ga_2S_3 [29] glasses as indicated in Fig. 5. And the β can be tailored from 1.16 to 104 $\times 10^{-10}$m/W, suggesting that the largest β variation range is achieved in sole glass system (i.e. GeS_2-Sb_2S_3) as far as we know.

4. Conclusion

We have investigated the optical properties of (100-x)GeS_2-xSb_2S_3 glasses, such as optical bandgap, linear refractive index, impurity absorption, and nonlinear optical response, within a large glass-forming region. It is found that the increase of Sb_2S_3 content with compositional variation of 0-90 mol% causes the decrease of optical bandgap from 2.70 to 1.67 eV, the increase of linear refractive index n from 2.1188 to 2.4458 for only 30 mol% variation of Sb_2S_3 content, and a large variation of nonlinear refractive index n_2 and nonlinear absorption coefficient β. Combined with the compositional dependence of impurity absorption bands in mid-IR spectral region, it is proposed that the big difference of bonding and microstructural arrangement between three-coordinated Sb species and four-coordinated Ge entities is responsible for these flexible properties. We believe that the GeS_2-Sb_2S_3 glasses with a large tailorable range of optical properties would be one of the most promising materials for applications in infrared spectral region.

Acknowledgments

This work was partially supported by the National NSFC (Grant No. 61108057) and the Zhejiang NSFC (Grant No. Y4110322), NSFC of Ningbo City (Grant No. 2011A610091). It also was sponsored by K.C. Wong Magna Fund in Ningbo University.

Reference

[1] C. Lin, L. Calvez, B. Bureau, H. Tao, M. Allix, Z. Hao, V. Seznec, X. Zhang and X. Zhao, Phys. Chem. Chem. Phys., **12**(15), 3780 (2010).
[2] C. Lin, H. Tao, R. Pan, X. Zheng, G. Dong, H. Zang X. Zhao, Chem. Phys. Lett., **460**(1-3), 125 (2008).
[3] C. Lin, H. Tao, X. Zheng, R. Pan, H. Zang, X. Zhao, Opt. Lett., **34**(4), 437 (2009).
[4] A. V. Kolobov, P. Fons, A. I. Frenkel, A. L. Ankudinov, J. Tominaga, T. Uruga, Nat. Mater., **3**(10), 703 (2004).
[5] H. Takebe, H. Maeda and K. Morinaga, J. Non-cryst. Solids, **291**(1-2), 14 (2001).

[6] H. Takebe, T. Hirakawa, T. Ichiki, K. Morinaga, J. Ceram. Soc. Jpn., **11**(8), 572 (2003).
[7] C. Lin, L. Calvez, M. Rozé, H. Tao, X. Zhang, X. Zhao, Appl. Phys. A - Mater., **97**, 713 (2009).
[8] C. Lin, L. Calvez, H. Tao, M. Allix, A. Moréac, X. Zhang and X. Zhao, J. Solid State Chem., **184**(3), 584 (2011).
[9] G. Dong, H. Tao, S. Chu, S. Wang, X. Zhao, Q. Gong, X. Xiao and C. Lin, Opt. Commun. **270**(2), 373 (2007).
[10] S. S. Uzun, S. Sen, C. J. Benmore, B. G. Aitken, J. Phys. Chem. C, **112**(18), 7263 (2008).
[11] H. Tichá, L. Tichý, N. Rysavá, A. Tríska, J. Non-cryst. Solids, **74**(1), 37 (1985).
[12] D. Svadlák, Z. Zmrhalová, P. Pustková, J. Málek, L. A. Pérez-Maqueda, M. Criado, J. Non-cryst. Solids **354**(28), 3354 (2008).
[13] J. Málek, Z. Zmrhalová, J. Barták, P. Honcová, Thermochim. Acta, **511**(1-2), 67 (2010).
[14] V. S. Shiryaev, J. Troles, P. Houizot, L. A. Ketkova, M. F. Churbanov, J. L. Adam and A. A. Sibirkin, Opt. Mater., **32**(2), 362 (2009).
[15] J. Shánelová, P. Kostál and J. Málek, J. Non-cryst. Solids, **352**(36-37), 3952 (2006).
[16] L. Cervinka, O. Smotlacha, J. Bergerová, L. Tichý, J. Non-cryst. Solids, **137-138**(Part 1), 123 (1991).
[17] L. Petit, N. Carlie, F. Adamietz, M. Couzi, V. Rodriguez, K. C. Richardson, Mater. Chem. Phys., **97**(1), 64 (2006).
[18] F. Chen, T. Xu, S. Dai, Q. Nie, X. Shen, X. Wang, B. Song, J. Non-cryst. Solids, **356**(50-51), 2786 (2010).
[19] L. Calvez, P. Lucas, M. Rozé, H. L. Ma, J. Lucas, X. H. Zhang, Appl. Phys. A - Mater., **89**(1), 183 (2007).
[20] H. Guo, H. Chen, C. Hou, A. Lin, Y. Zhu, S. Lu, S. Gu, M. Lu and B. Peng, Mater. Res. Bull. **46**(5), 765 (2011).
[21] T. S. Kavetskyy, A. P. Kovalskiy, V. D. Pamukchieva O. I. Shpotyuk, Infrared Phys. Techn., **41**(1), 41 (2000).
[22] V. S. Shiryaev, L. A. Ketkova, M. F. Churbanov, A. M. Potapov, J. Troles, P. Houizot, J. L. Adam, A. A. Sibirkin, J. Non-cryst. Solids **355**(52-54), 2640 (2009).
[23] M. Sheik-Bahae, A. A. Said, T. H. Wei, D. J. Hagan, E. W. Van Stryland, IEEE J. Quantum Elect. **26**(4), 760 (1990).
[24] K. Tanaka, Appl. Phys. Lett., **80**(2), 177 (2002).
[25] L. Petit, N. Carlie, K. Richardson, A. Humeau, S. Cherukulappurath and G. Boudebs, Opt. Lett. **31**(10), 1495 (2006).
[26] J. M. Harbold, F. O. Ilday, F. W. Wise, B. G. Aitken, IEEE Photonic. Tech. L., **14**(6), 822 (2002).
[27] M. Sheik-Bahae, D. C. Hutchings, D. J. Hagan, E. W. Van Stryland, IEEE J. Quantum Elect., **27**(6), 1296 (1991).
[28] S. Kasap, P. Capper, Springer Science+Business Media, Inc. (2006).
[29] G. Dong, H. Tao, X. Xiao, C. Lin, Y. Gong, X. Zhao, S. Chu, S. Wang and Q. Gong, Opt. Express, **15**(5), 2398 (2007).

*Corresponding author: linchanggui@gmail.com